SUPPLEMENTARY METHODS

Primary Adult Hippocampal Stem Cell Cultures

Primary neural stem/progenitor cells (NPCs) were isolated from the dentate gyrus of 11- to 14-week-old male wild-type mice as described previously (1, 2). Briefly, mice were euthanized with isoflurane, the brain was cut into 400 μm sections using tissue chopper (McIlwain Tissue Chopper, 10180), and placed in Hank's Balanced Salt Solution (HBSS; 14025-126, Invitrogen/Gibco) containing 30 mM glucose, 2 mM HEPES, 26 mM NaHCO3. The DG was isolated and dissociated using the MACS® Neural Tissue Dissociation Kit (130-092-628, Miltenyi Biotec) and finally resuspended in 1 ml of Initial Proliferation Medium (IPM) into one well of a 24-well tissue culture plate (3524, Corning Costar). IPM media is made up with Neurobasal medium (21103-049, Invitrogen/Gibco), B27 supplement (17504-044, Invitrogen/Gibco), GlutaMAX (35050061, Gibco), Pen/Strep (30-001-Cl, Corning), 20 ng/ml of human Fibroblast Growth Factor-2 (FGF-2) (100-18B, PeproTech), and human Epidermal Growth Factor (EGF) (AF-100-15, PeproTech) and then plated. For propagation, we used cell proliferation media made with DMEM/F12 media (DM-25, Omega), N2 supplement (N2; 17502-408, Invitrogen/Gibco), L-Glutamine (2503-081, Invitrogen/Gibco), Pen/Strep, FGF-2, and EGF peptides. For differentiation, we used only early passage cells (between passages 4 and 10). Differentiation of NPCs to neurons and astrocytes was carried out as described. Neurospheres were disassociated with trypsin and plated in 6 well (3516, Corning Costar) plates coated with poly-L-ornithine (P-3655, Sigma) and laminin (354232, BD Biosciences) at the density of 1 × 105 cells/wells. Chamber slides (80827, Ibidi) were used for STORM experiments. At 24 h post-plating, differentiation was initiated by replacing media with differentiation media, containing retinoic acid (1 μM, R-2625, Sigma) and forskolin (1 μM, F-6886, Sigma), which was partially replaced daily.

Stereotaxic Surgery

On the third day of housing in their respective conditions, mice were anesthetized with 3% isoflurane, and stereotaxic surgery was performed to deliver one μl of the virus, into the dorsal and ventral dentate gyrus of both hemispheres using spatial coordinates relative to bregma as follows: Dorsal dentate gyrus, anterior-posterior (AP) = −2.10 mm; medial-lateral (ML) = 1.9 mm; dorsoventral (DV) = −2.20 mm, and ventral dentate gyrus, AP = −3.10 mm; ML = 2.8 mm; DV = −3.20 mm. These coordinates were modified from the mouse brain atlas and adjusted for six-week-old mice. Tissues from mice injected with retroviral vectors for morphological analysis and single nuclei isolation were collected 28 days later (3). Mice injected with AAV8-GFP or AAV8-irisin-FLAG were harvested at the end of behavior studies.

Behavioral Assays

Open field test (OPF)

For the open field test (OPF) (4), mice were placed individually in an open field arena (27.3 × 27.3 cm, height 20.3 cm) housed within a sound-attenuating cubicle (Med Associates, Inc., St. Albans, VT) and permitted to move freely. Trials lasted 30 or 60 minutes with a five-minute time bin as specified in each experiment. Animal motion and cumulative path length were automatically tracked via 2X and 1 Z 8-beam IR arrays and recorded by Activity Monitor software (Version 4.0, Med Associates, Inc., St. Albans, VT). Mean substitution of distance traveled was used for incomplete measurements when mice escaped the open field box.

Rotarod test

Motor function was evaluated with a five-station accelerating rotarod stand-alone for mice (Ugo Basile, Italy). Two animals were tested at the same time. Each animal performed two consecutive five-minute trials a day with 30 minutes inter-trial interval. The trials commenced with the mouse situated on the rod rotating at 4 rpm for 5 minutes, and the rod was then set in motion with an accelerating speed of 4 to 40 rpm. The latency to the first fall during the two consecutive five-min trials was recorded and averaged(4).

Grip strength test

The Grip Strength Meter (Ugo Basile, Italy) was used to measure forelimb grip strength (5). As a mouse grasped the bar, the peak pull force in N was recorded on a digital force transducer. In the test, a mouse was allowed to grab the bar mounted on the force gauge. The gauge was reset to 0 N after stabilization, and the mouse's tail was slowly pulled back. The gauge recorded tension at the time the mouse released its forepaws from the bar. A total of 5 trials were done for each mouse.

Tail suspension test (TST)

The tail suspension test (TST) was carried out according to the method described previously (6). Each mouse was suspended for 6 min by the tail (2 cm from the end of the tail) using adhesive tape. After the first 2 min of the test, the total duration

of immobility (in seconds) was measured using software (Med Associates, VT). An animal was judged to be immobile when it ceased moving limbs and body, making only movements to breathe.

Elevated plus maze (EPM)

The elevated plus maze (EPM) consisted of two open and two closed (30 cm long and 5 cm wide) arms extended out from a central platform 85 cm above the floor. The test was carried out in dim ambient lighting. Mice were placed near the center compartment of the maze, facing an open arm, and allowed to explore the apparatus for 5 minutes. A computer-assisted video-tracking system (TopScan software, CleverSys Inc., Reston, VA) was used to record the number of open and closed arm entries as well as the total time spent in open, closed, and center compartments. An increase in the percent time spent or entries into the open arms was used as a surrogate measure of anxiolytic-like behavior (7).

Gait analysis

To measure gait and motor coordination, mice were tested on the TreadScan system (hardware: Columbus Instruments; Columbus, OH; software GaitScan, CleverSys, Reston, VA). A high-speed digital video camera was mounted to record the ventral view of a clear treadmill belt reflected off a mirror. An adjustable compartment was mounted over the treadmill belt, ensuring that the mouse remained in the view of the camera. The treadmill was set to 13cm/sec and video recorded for approximately 24 sec. TreadScan software automatically extracted optimal video segments and analyses that provided measures of stride timing, range of motion, inter-foot distance, and coordination (4).

Morris water maze (MWM)

In the Morris water maze (MWM), mice were trained to find the hidden platform (15 cm diameter) in the maze (1.4 m diameter) (8, 9). The water was made opaque using nontoxic white paint (00011-1009, Blick Art Materials) and the temperature was maintained at 25^0C. Mice were trained for 6-9 consecutive days with 2 or 4 trials per day. Starting points were changed daily for each trial. The animals were allowed a maximum of 60 s to locate the platform with a ten-minute inter-trial interval. A 60 s probe trial was performed at the indicated time points after the training. For reversal, the platform was moved to the opposite quadrant, and mice were trained to find the hidden platform following the same trial protocol as the acquisition described above. Probe trials were performed at indicated time points after the training. Data collection and analysis were performed using the ANY-maze tracking system (Stoelting Co. Wood Dale, IL). Latency, time spent in the correct quadrant, swim distance, and swim speed were calculated.

Contextual fear conditioning (CFC)

Contextual fear conditioning (CFC) was used to assess memory and is based on the tendency of mice to show a fear response (freezing) when re-exposed to the context where they received an aversive stimulus (in this case, foot shock). Mice were placed into a conditioning chamber (17 cm length × 17 cm width × 25 cm height, Maze Engineers Stokie, IL) with Plexiglas sidewalls, and a floor consisting of steel bars. Mice were allowed to explore the chamber for 2 min and were given 2 presentations of a 2 s foot shock (0.5 mA) separated by 2 min. Mice were removed from the chamber 1 min after the last foot shock. Twenty-four hours after the training session, mice were placed back into the conditioning chamber for 3 min (no electric shock was delivered during this session). and freezing was videotaped and scored with ANY-maze software (Stoelting Co. Wood Dale, IL). The freezing response was used as a surrogate marker of memory performance because the memory of receiving the shock, during the training session in context A on day 1, is expected to induce significant freezing episodes during the day 2 session. Mice that did not freeze after receiving the shocks on day 1 were excluded from that analysis as we cannot use freezing as a proxy for learning or memory (7).

Contextual Fear Conditioning Discrimination Learning (CFC-DL)

For Contextual Fear Conditioning Discrimination Learning (CFC-DL) we used the same setup as CFC describes above and followed a modified protocol described previously (10). For the training context (designated context A), the cubicle door was closed, the fan and house light were on, stainless-steel bars were exposed, and each conditioning chamber was cleaned with 70% ethanol and Windex for Plexiglas between each trial. Context B was a modified version of A with black and white checkered wall panels, the fan and house lights were on, stainless-steel bars were exposed, and the cubicle door was left ajar during the test. The training days 1,3-5 and 7-9 of our CFC discrimination paradigms (CFC-DL) protocol consisted of delivering a single 2 s foot shock of 0.5 mA at 180 s after placement of the mouse in the training context A. The mouse was taken out 15 s after termination of the foot shock. On days 2, 6, 10, 50% of the animals were first tested in context A or B in the morning and context B or A in the afternoon session. No foot shock was administered during the test sessions in either context on these days. Mice were allowed to rest for 4 hours between tests. Freezing behavior over the initial 180 s was used to assess discrimination between both contexts. For the APP/PS1 mice, the CFC-DL followed a modified protocol described previously (11). Mice were exposed to contexts A and B every day, in alternating orders, with 4hr rest between

context exposure, for ten days. As described above, in context A the mice received a 2s foot shock and in context B no foot shock was administered, and freezing was assessed throughout. Mice that did not freeze after receiving the shocks on day 1 were excluded from that analysis as we cannot use freezing as a proxy for learning or memory (12).

Novel Object Recognition (NOR)

The Novel Object Recognition (NOR) Test was used following the methods described previously with modifications (13). Briefly, we used a white plastic chamber with a dimension of 60 cm-long, 40 cm-wide, and 40 cm-high. Legos and Blocks with different colors and shapes were used as familiar and novel objects. Two boxes were used in parallel. Data collection was performed using the ANY-maze tracking system (Stoelting Co. Wood Dale, IL). Each mouse underwent 5 days of the protocol. On the first day, all mice were acclimated to the empty arena for 10 minutes. In the next 3 days of training, the mice were exposed to the same chamber, which now contains 2 identical objects, for 10 minutes (training 1-3). On the fifth day, each mouse was placed back in the arena with the same object and a novel object for an additional 10 min test session (Test). The amount of time interacting with the objects was recorded and calculated as percent time interacting with familiar vs novel objects. Mice that spend less than ten seconds interacting with the objects were excluded since low exploratory activity biases the analysis (14).

Spontaneous alternation behavior (SAB)

Spontaneous alternation behavior (SAB) tests were conducted in a Y-maze. Each arm of the Y-maze was 35 cm long, 5 cm wide, and 10 cm high. To reduce anxiety in the animals, light in the testing area was dimmed to 50 lux. Mice were handled for three days before testing. This test consisted of a single 5 min trial, in which the mouse was allowed to explore all three arms of the Y-maze. If a mouse climbed on the maze walls, it was immediately returned to the abandoned arm. The start arm was varied between animals to avoid placement bias. Spontaneous Alternation [%] was defined as consecutive entries in 3 different arms (ABC), divided by the number of possible alternations (total arm entries minus 2). Re-entries into the same arm were rated as separate entries. Mice with less than 8 arm entries during the 5-min trial were excluded from the analysis as significantly lower exploratory activity biases the analysis. (15).

Barnes Maze

The Barnes maze test was performed as previously described (16). Briefly, a large circular maze containing 20 holes was centered over a pedestal and elevated approximately 90 cm above the floor (60170, Stoelting Co.). The escape hole consisted of a small dark recessed chamber under the platform that was similar in texture and color to the maze. Distinct visual cues were placed at four equally spaced points around the room. An overhead light provided additional motivation to find the escape hole. Following two-minute habituation on the platform, the training days proceeded over a period of 4 days, with four trials on each day for each mouse. Mice were given 180 s for each trial to identify the escape hole by jumping in or identifying the hole with extended/overt head pokes. If mice failed to identify the escape hole within the allotted 180 s, they were gently guided by light tapping/directing towards the escape hole and scored at the allotted investigation time. For each trial within a day, the starting location for the mouse was rotated relative to the escape hole position. Mice were trained with 20 minutes intertrial intervals. Between each trial, the maze and escape hole were thoroughly cleaned with 70% ethanol to remove any cues that might affect performance in subsequent trials. On the probe trial day 5, the escape box was removed, and mice were allowed to explore the platform for 90 s.

BrdU and EdU labeling

Mice were injected daily intraperitoneally (i.p.) with BrdU (50 mg /kg, (Sigma, dissolved in 0.9% saline,) or EdU (50mg/kg, Abcam, dissolved in PBS). Solutions were filtered at 0.22 µm. EdU was dissolved in 1x PBS and filtered at 0.22 µm. At the end of the experiment, the mice were anesthetized with isoflurane and perfused transcardially. For running experiments, mice received five daily injections of EdU after three days in the wheel. For the running-induced c-Fos activation assay, mice received ten daily injections of BrdU after one day in the wheel. On day 31, the brains were collected four hrs into the dark cycle. For the baseline neurogenesis studies, mice received ten daily injections of BrdU and tissues were collected 30 days after the last injection. For AAV8 experiments with WT, F5KO, APP/PS1, and 5xFAD mice, the animals received ten daily injections of BrdU, and tissues were collected at the end of behavior studies.

Immunohistochemistry and microscopy

Immunofluorescence (IF) and immunohistochemistry (IHC) staining were done following the methods described previously (17). Brains fixed in 4% PFA were cryoprotected in 5%, 10%, and 30% sucrose gradient for 24 hrs or until they sunk in the bottom and embedded in Tissue-Tek O.C.T. (QIAGEN). Staining was done using 35 µm coronal free-floating sections (one-in-six series) from embedded tissue. For IF for GFP, 3D6, FLAG, GFAP, IBA1, MAP2, aVb3 integrins, and aVb5 integrin,

sections (tissue) or coverslips (cells) were washed in PBS, blocked (PBS with 0.1% Triton X-100, 10% normal goat serum), and incubated in the primary antibody at 4°C overnight followed by secondary antibodies incubation for two hours after PBS wash for 15 minutes. Nuclei were counterstained using Hoechst 33342 (Thermo Fisher Scientific). For BrdU IF, sections were incubated for two hrs in the 50% formamide/2X SSC (0.3 M NaCl and 0.03 M sodium citrate) at 65°C followed by 15 min in 2X SSC buffer. After that sections were incubated in 2 N HCl at 37°C for 30 minutes to denature the DNA. 0.1 M boric acid (pH 8.5) followed by several washes in Tris-buffered saline (TBS, pH 7.5) were used to neutralize the acid, and then the usual IF protocol described above was followed. For BrdU/c-Fos/NeuN triple staining sections were incubated in primary antibodies for 48h after denaturing the DNA without incubation with SSC. BrdU IHC was completed using the ABC peroxidase complex (ABC Kit, Vector Laboratories) with the chromogen 3,3′-diaminobenzidine (DAB) (Sigma) following the manufacturer protocol. Before imaging sections were mounted on gelatin-coated slides, air-dried, dehydrated, cleared, and coverslipped. To label sections for EdU-positive cells, we used the Click-iT EdU Cell Proliferation Kit (Invitrogen) as described previously(18).

For antigen retrieval of BrdU in IF, brain sections were incubated for two hours in 50% formamide/2X SSC (0.3 M NaCl and 0.03 M sodium citrate) at 65°C followed by a 15 min wash in 2X SSC buffer. After washing, the sections were incubated in 2N HCl at 37°C for 30 minutes followed by neutralization with 0.1 M boric acid (pH 8.5) and several washes in TBS (pH 7.5). The usual IF protocol was resumed after these steps.

Glial cell and amyloid plaque quantification

For glial cell quantification, matching-bregma sections were used across all mice for microglia and astrocyte morphological quantification. Images were taken at a 20X magnification using a slide scanner (Zeiss Axio Scan.Z1). Images were reconstructed using ImageJ (v2.0.0-rc-69/1.53c) software. Once the respective fluorescent channel, microglia, and astrocytes were isolated, a binary image was created using a previously described protocol (19). A square (ROI) of 200 µm x 200 µm (0.04 mm2) was outlined in the DG, CA1, and CA3 regions, respectively. Within each ROI, the total number of positive cells was manually quantified. Three cells from each ROI were selected to measure morphological differences, including area, circularity, and Feret value.

The amyloid plaques (staining with 3D6 antibody) were captured with 20X magnification using a slide scanner (Zeiss Axio Scan.Z1) and quantified using ImageJ (v2.0.0-rc-69/1.53c) software. The hippocampal area on each section was outlined as regions of interest (ROI) and thresholded to quantify the percentage area occupied by the plaques. Ten to twelve sections per mouse were averaged. For the cortex, three ROIs of 500 µm x 500 µm squares (0.25mm^2) were outlined per section, thresholded to quantify the area occupied by the plaques, and then the average was calculated. Six sections of matching-bregma per mouse were used.

Morphological analysis

Dendritic complexity and spine morphology were analyzed following the methods described previously (20). Briefly, sections were imaged using confocal microscopy (LSM 780 Carl Zeiss, Germany) with a 20X objective and step size of 1 µm. Imaging was focused on the suprapyramidal blade of the DG in dorsal and ventral hippocampal slices. For Sholl analysis, neurons were traced using the Simple Neurite Tracing plugin from ImageJ (v2.0.0-rc-69/1.53c). Each tracing was analyzed for soma size, apical dendrite length, and branch points. The total dendritic length was defined as the summed length of all branches in the apical dendrite. At least five neurons per animal were analyzed.

For quantification of dendritic spines of retroviral injected or Thy1-GFP+/F5KO brain sections, confocal z-stack images were acquired using a Leica DMI8-CS SP8 confocal research microscope. Imaging was performed using a 63X objective, plus 2X optical zoom and 4X digital zoom. For spine imaging, confocal z-stacks (2048 x 2048 resolution) with 0.3 µm step size were taken from top to bottom to cover all spines centered on a selected dendritic segment. Z-stacks were flattened using the maximum intensity projection, and flattened images were quantified using ImageJ (v2.0.0-rc-69/1.53c). For spine density, spines were counted manually for at least 100 µm of dendritic length per region per mouse. Spine head diameter (at the widest point of the spine head) and spine length (from dendrite to the furthest point of the spine head) were measured manually. More than 150 spines were analyzed per region per mouse to calculate spine size distribution (RV injected newborn neuron, dorsal 3983 and ventral 4431 spines, Thy1-GFP+/F5KO mature granule cells, dorsal 1869 and ventral 1887 neurons). The outer molecular layer was defined as the 1/3 of the molecular layer furthest from the granule cell layer, while the inner molecular layer was defined as the 1/3 of the dendritic tree closest to the granule cell layer.

Electrophysiological Analysis

Electrophysiological analysis was performed according to the protocol described previously (21, 22) with slight modifications. Adult male animals (8 weeks) were anesthetized with isoflurane and rapidly decapitated. The brains were removed and immersed in ice-cold artificial cerebrospinal fluid (ACSF) containing (in mM): 125 NaCl, 2.50 KCl, 1.25 NaH2PO4, 25.0 NaHCO3, 2.00 CaCl2, 1.30 MgCl2, and 10.0 dextrose, oxygenated with 95%O2/5%CO2. Transverse hippocampal slices (350 μm) were generated using a Vibratome Sectioning System 1500 (Ted Pella, Redding, CA, USA). Slices were gently transferred to an incubation chamber filled with oxygenated ACSF and maintained at 32°C for a minimum of 1h post dissection. Slices were transferred to a recording chamber and superfused at a 1–2 mL/min rate with 32°C, oxygenated ACSF. A concentric bipolar stimulating electrode (FHC, Bowdoin, ME, USA) was placed under visual guidance into the medial performant path (MPP) of the DG molecular layer using an Olympus BX51W1 microscope (Center Valley, PA, USA).

Borosilicate recording electrodes (0.7–1.5 MΩ) filled with ACSF were placed in the MPP of the DG molecular layer. Field excitatory postsynaptic potentials (fEPSPs) were evoked using monophasic negative current pulses (120 μs, 10–40 μA) supplied via a digital stimulus isolation unit (Getting Instruments, San Diego, CA, USA). Responses were acquired at 100 kHz using a MultiClamp 700B amplifier (Molecular Devices, Sunnyvale, CA, USA). For each slice, stimulus intensity was adjusted to yield 50–55% of the maximal response slope (without population spikes). Baseline measurements were collected using individual fEPSPs evoked every 15 s. After a steady baseline of 15 min, a paired-pulse protocol and an input-output (I/O) protocol were applied to evaluate possible changes in synaptic transmission. Paired-pulse experiments consisted of applying 6 sets of 2 pulses each with a 50 ms interpulse interval (15 s between paired stimuli), and a ratio was calculated by dividing the slope of the second fEPSP by the first. I/O curves were generated by measuring fEPSP amplitude in response to increasing stimulation (0.03-0.3 ms pulse width). To induce LTP in the DG, slices were exposed to the GABAA receptor antagonist bicuculline methiodide during baseline recordings (5 μM, washed for 20 min, Sigma, MO, USA). This protocol allows for a significant reduction in tonic inhibition and isolation of the excitatory component of synaptic transmission in the DG. LTP was induced by applying a high-frequency stimulus (HFS; 4 trains of 50 pulses at 100 Hz, 30 s apart), and responses were recorded for 60 minutes after the conditioning stimulus. fEPSPs slopes were calculated using Clampfit 10 (Molecular Devices). Potentiation was quantified by examining the average of the last 5 min of the postconditioning baseline (55–60 min). Slices obtained from the septal pole until the first half of the hippocampus were defined as the dorsal hippocampus, while the remaining half of the slices were defined as the ventral hippocampus (23).

Isolation, FACS sorting, and RNA-sequencing of nuclei of newborn neuron

Mice were placed individually in either a cage with or without a running wheel. On day two, mice were stereotaxically injected with RV-SYN-GTRgp. Twenty-eight days later, were euthanized with isoflurane and the hippocampi were micro-dissected in ice-cold HBSS (Gibco). The nuclei were isolated as described previously with modifications (24). Tissue samples (< 0.5 cm size) were homogenized using a glass Dounce tissue grinder (D8938, Sigma) (20 times with pastel A, and 20 times with pastel B) in two ml of ice-cold EZ PREP (NUC-101, Sigma) and incubated on ice for five minutes, with additional two ml ice-cold EZ PREP. Nuclei were then filtered through a 70 and 35 μm cell strainer (130-098-458, MACS ® SmartStrainer) and centrifuged at 500 x g for five minutes at 4°C. The nuclei were washed in eight ml Nuclei Suspension Buffer (NSB; consisting of RNAse-free 1X PBS, 1% BSA (RNAse free, B6917, Sigma), and 0.1% RNAse inhibitor (2313A, Clontech)). Following another centrifugation at 500 x g for five mins at 4°C, the isolated nuclei were resuspended in 300 μl NSB with Vybrant Ruby dye (1:700 dilution) (Vybrant DyeCycle Ruby Stain, #V-10309, Thermo Fisher Scientific, MA). Nuclei were kept on ice until sorting using Fluorescence Activated Cell Sorting (MGH Pathology: Flow, Image, and Mass Cytometry Core, CNY, BD FACSAria Fusion Cell Sorter) into a chilled Eppendorf tube with NBS buffer. FACS gating was set on FSC, SSC, and on fluorescent channels to include only Ruby+ or Ruby+/GFP+ nuclei (for nuclei tagged by GFP expression of the newborn neurons) as depicted in Extended Data Fig. 4. The FACS gates for sorting were set using a negative control sample (WT non-GFP injected tissue). Representative plots were generated with FlowJo version 10.7.1 software. The collected nuclei were spun down at 500 x g for five mins at 4°C and the pellet was stored at -80°C.

Library Preparation, Sequencing, Bioinformatic analysis were performed at the Dana-Farber Cancer Institute Molecular Biology Core Facilities. cDNA was synthesized from sorted cells using Takara SmartSeq v4 reagents according to manufacturer's protocol with the following modification: 1μl of 2X Reaction buffer was used with 1μl of CDS primer and 18 cycles of PCR were used for the cDNA amplification step. Full-length cDNA was fragmented to a mean size of 150bp with a Covaris M220 ultrasonicator and Illumina libraries were prepared from 2ng of sheared cDNA using Rubicon Genomics Thruplex DNAseq reagents according to the manufacturer's protocol. The finished dsDNA libraries were quantified by Qubit fluorometer, Agilent TapeStation 2200, and RT-qPCR using the Roche Kapa library quantification kit.

Uniquely indexed libraries were pooled in equimolar ratios and sequenced with single-end 75bp reads on an Illumina NextSeq500 run by the Dana-Farber Cancer Institute Molecular Biology Core Facilities. Sequenced reads were aligned to the UCSC mm10 reference genome assembly and gene counts were quantified using STAR (v2.5.1b) (25). Differential gene expression testing was performed by DESeq2 (v1.10.1) (26). Normalized read counts (FPKM) were calculated using cufflinks (v2.2.1)(27). RNAseq analysis was performed using the VIPER snakemake pipeline(28). Pathway analysis was performed using DAVID(29, 30) and GSEA(31, 32).

RNA-seq of dentate gyri from F5KO and WT mice

Library preparations, and sequencing reactions were conducted by the Dana-Farber Cancer Institute Molecular Biology Core Facilities. Libraries were prepared from 500 ng of purified total RNA using the Illumina TruSeq stranded mRNaseq kit according to the manufacturer's protocol. Libaries were quntifiied using a Qubit fluorometer. Pooled in equimolar ratios, uniquely indexed libraries were sequenced on an Illumina NextSeq500 with single-end 75-bp reads.

RNA-seq of hippocampal tissue from APP/PS1 mice injected with AAV8-Irisin-FLAG

RNA extraction, library preparations, and sequencing reactions were conducted at GENEWIZ, LLC. (South Plainfield, NJ, USA. Total RNA was extracted from fresh frozen tissue samples using Qiagen RNeasy Plus Universal mini kit following the manufacturer's instructions (Qiagen, Hilden, Germany). Extracted RNA samples were quantified using Qubit 2.0 Fluorometer (Life Technologies, Carlsbad, CA, USA) and RNA integrity was checked using Agilent TapeStation 4200 (Agilent Technologies, Palo Alto, CA, USA). RNA sequencing libraries were prepared using the NEBNext Ultra RNA Library Prep Kit for Illumina following the manufacturer's instructions (NEB, Ipswich, MA, USA). Briefly, mRNAs were first enriched with Oligo(dT) beads. Enriched mRNAs were fragmented for 15 minutes at 94 °C. First strand and second-strand cDNAs were subsequently synthesized. cDNA fragments were end-repaired and adenylated at 3'ends, and universal adapters were ligated to cDNA fragments, followed by index addition and library enrichment by limited-cycle PCR. The sequencing libraries were validated on the Agilent TapeStation (Agilent Technologies, Palo Alto, CA, USA), and quantified by using Qubit 2.0 Fluorometer (Invitrogen, Carlsbad, CA) as well as by quantitative PCR (KAPA Biosystems, Wilmington, MA, USA). The sequencing libraries were clustered on 1 lane of a flowcell. After clustering, the flowcell was loaded on the Illumina HiSeq instrument (4000 or equivalent) according to the manufacturer's instructions. The samples were sequenced using a 2x150bp Paired-End (PE) configuration. Image analysis and base calling were conducted by the HiSeq Control Software (HCS). Raw sequence data (.bcl files) generated from Illumina HiSeq was converted into fastq files and de-multiplexed using Illumina's bcl2fastq 2.17 software. One mismatch was allowed for index sequence identification.

Differential Expression analysis

Per-sample transcript-level quantifications (read counts and transcripts per million; TPM) are processed and aggregated to the gene-level using tximport (V 3.13, Bioconductor), a R/Bioconductor package. Gene-level counts are filtered to retain contributions from more useful biotypes (which may be named differently depending on the species), broadly these include protein_coding, lncRNA, macro_lncRNA, miRNA, antisense, pseudogene, processed_pseudogene, processed_transcript, transcribed_processed_pseudogene, transcribed_unprocessed_pseudogene. Genes are further filtered to remove those with no counts in any sample. Per-sample gene-level read counts for genes surviving the above filters are normalized using the DESeq2 (v1.10.1), R/Bioconductor package. DESeq2 is also used to model expression differences and assess the significance of coefficients of interest via a Negative Binomial generalized linear model and using Wald tests to identify differentially expressed (DEX) genes in these contrasts. Nominal p values are corrected using the method described by Benjamini and Hochberg (33) and DEX genes are those that achieve a BH-corrected $p < 0.05$. Further interrogation/plotting of DEX genes is enabled by the following R packages: data wrangling using tidyverse; plotting multi-way intersections using UpSetR; plotting heatmaps using pheatmap; volcano plots using EnhancedVolcano.

Direct stochastic optical reconstruction microscopy (dSTORM)

Two-color dSTORM experiments were performed using a Nikon system (Ti2 Eclipse/STORM 5.0) with an HP APO TIRF AC 100x/1.49 NA oil objective and ORCA-Flash4.0v2 S-CMOS camera (Hamamatsu Photonics) and NSTORM quadband filter, and 405, 488, 561, and 647 nm lasers. Cells were prepared(34), probed with primary antibodies overnight, and then incubated with in-house prepared conjugated secondary antibodies, donkey anti-rabbit Alexa Fluor 647 and donkey-anti-mouse Alexa Fluor 488 (3 μg/mL), for 60 min at RT in the dark(35). To reduce photobleaching, an imaging buffer with 100 mM 2-mercaptoethanolamine (MEA) and 1% (v/v) GLOX (glucose oxidase and catalase solution) was used. For each dye, 15,000 frames were acquired with a 30 ms exposure time. NIS Elements 5.0 (Nikon Instruments) was used to identify localization. To quantify colocalization of individual proteins and molecules (localizations) in regions of interest (ROI), drawn around the whole cell, Clus-DoC(36) was utilized and a custom script was used to determine the output. To determine

the relative changes in clustering robustly, we did not utilize a grouping algorithm as grouping can lead to undercounting and reduced dSTORM detection efficiency (37). We only considered clusters having at least five localizations for integrin aVb3, integrin aVb5, and irisin-FLAG.

Supplementary Data Tables

Supplementary data table 1: List of primary antibodies

Antibody	Company/Origin	Catalog number	Isotype	Application	Dilution	Clone	Lot	Reference/Validation
Mouse Anti-Integrin αVβ3	Abcam	Ab78289	IgG1	ICC	1:100	27.1 (VNR-1)	GF3214190-1	Kim, H. *et al*., Cell, 2018(38)
Mouse Anti-Integrin αVβ5	Millipore	MAB1961	IgG1	ICC	1:100	P1F6	3284341	Kim, H. *et al*., Cell, 2018(38)
Chicken Anti-NeuN	Millipore	ABN91	IgY	IF	1:500	Polyclonal	3458259	Black, BJ. *et al*., Front Cell Neurosci, 2017(39)
Rabbit Anti-c-Fos	Abcam	Ab190289	IgG	IF	1:10,000	Polyclonal	GR3332124-2	Everard, A. *et al*., Nat Commun, 2019(40)
Rabbit Anti-Glial Fibrillary Acidic Protein (GFAP)	Millipore	Ab5804	N/A	IF	1:500	Polyclonal	3429094	Ma, SM. *et al*., PloS one, 2015(41)
Chicken Anti-GFAP	Abcam	Ab4674	IgY	IF	1:1000	Polyclonal	GR3234435-4	Markowitz, JE. *et al*., Cell, 2018(42)
Anti-Iba1, Rabbit	Wako	019-19741	N/A	IHC	1:1000		PTK1381	Choi, SH. *et al*., Science, 2018(17)
Rat Anti-BrdU	Abcam	Ab6326	IgG2a	IF	1:500	BU1/75 (ICR1)	GR3289293-1	Choi, SH. *et al*., Science, 2018(17)
Chicken Anti-MAP2	Abcam	Ab5392	IgY	ICC	1:500	Polyclonal	GR3297672-3	Velasco, S. *et al*., Nature, 2019(43)
Mouse Anti-Aβ 3D6	Gift from Eli Lilly to Choi lab (Choi et al., 2018)	N/A	IgG1	IF	1:1000	Monoclonal	N/A	Choi, SH. *et al*., Science, 2018(17)
Rabbit Anti-DYKDDDDK Tag	Cell Signaling Technologies	14793S	IgG	IF/ELISA/WB	1:1000	D6W5B	5	Hoshino, A. *et al*., Nature, 2019(44)
Anti-Human Irisin/FNDC5	R&D	MAB8880	IgG1	ELISA	1:500	Monoclonal	CKBN0121011	Validated in house using recombinant irisin-FLAG (Adipogen, AG-40B-0136-C010)

Supplementary data table 2: List of Secondary antibodies

Antibody	Company/Origin	Catalog number	Isotype	Application	Dilution
Biotin-sp-conjugated Donkey anti-rat IgG (H+L)	Jackson ImmunoResearch Labs	712-065-153	IgG	IHC	1:200
Goat anti-rat Alexa Fluor488	Abcam	Ab150157	IgG	IF	1:500
Goat anti-rabbit Alexa Fluor555	Invitrogen	A21428	IgG	IF	1:500
Goat anti-chicken Alexa Fluor647	Invitrogen	A21449	IgG	IF	1:800
Goat anti-rabbit Alexa Fluor488	Invitrogen	A11008	IgG	IF	1:500
Goat anti-mouse Alexa Fluor647	Invitrogen	A21240	IgG	IF	1:500
Donkey anti-rabbit Alexa Fluor 647	In-house made Method described in detail (Schmider, AB. *et al*., J. Biol. Chem. 2020)(35)	Full-length antibody: 711-005-152 (Jackson ImmunoResearch Labs) Alexa Fluor 647: A200006 (Life Technologies)	IgG	STORM	3 ug/ml
Donkey-anti-mouse Atto 488	In-house made Method described in detail (Schmider, AB. *et al*., J. Biol. Chem. 2020)(35)	Full-length antibody: 715-005-150 (Jackson ImmunoResearch Labs) Atto 488: 41698 (Sigma-Aldrich)	IgG	STORM	3 ug/ml
Amersham ECL HRP-conjugated donkey anti-rabbit antibody	Cytiva	NA934	IgG	WB	1:5000

Supplementary data table 3: List of primers

Primer name	**Primer Sequence**	**Primer name**	**Primer Sequence**
Rsp18 Forward	CCTCACGCAGCTTGTTGTCTA	*Cebpb* Forward	CGAGGCTCACGTAACCGTAGT
Rsp18 Reverse	CATGCAGAACCCACG ACAGTA	*Cebpb* Reverse	ACGACTTCCTCTCCGACCTCT
Fndc5_nt Forward	CTGGAGGATGAAGTGGTCATTG	*Pgc1α* Forward	TGATGTGAATGACTTGGATACAGACA
Fndc5_nt Reverse	TGGTGTTCACCTCCTGAATG	*Pgc1α* Reverse	GCTCATTGTTGTACTGGTTGGATATG
Map2 Forward	GTCCAGCGTGGCATCACCCC	*Mef2a* Forward	AACCCAGGGAGTTCACTCGT
Map2 Reverse	TGCTTAGCAAGCGCCGCAGT	*Mef2a* Reverse	CATGCTCGAATCTGCTAATGTTG
Dcx Forward	ACATGACCACCTGGAGCAAG	*Mef2c* Forward	CCTGCTGGTCTCACCTGGTAA
Dcx Reverse	AGAAGCCCTTGGTGTGATGG	*Mef2c* Reverse	GAACGCGGAGATCTGGCTTA
Gfap Forward	ATTGCTGGAGGGCGAAGAAA	*Mef2d* Forward	AGGAAAAAGATTCAGATCCAGCG
Gfap Reverse	CTTTTGCCCCCTCGGATCT	*Mef2d* Reverse	GCGGTTCCGTTCATCAGTG
Aif1 Forward	GGAAAGTCAGCCAGTCCTCC	*Ucp1* Forward	CTTTGCCTCACTCAGGATTGG
Aif1 Reverse	TCACTTCCACATCAGCTTTTGA	*Ucp1* Reverse	ACTGCCACACCTCCAGTCATT
Igf1 Forward	CCTGCACTTCCTCTACTTGTGTTC	*Dio2* Forward	TGAACCAAAGTTGACCACCAG
Igf1 Reverse	CCACACTGACATGCCCAAGA	*Dio2* Reverse	CAGTGTGGTGCACGTCTCCAATC
Cidea Forward	GCCGTGTTAAGGAATCTGCTG	*Cytc* Forward	TTGTTGGCATCTGTGTAAGAGAATC
Cidea Reverse	TGCTCTTCTGTATCGCCCAGT	*Cytc* Reverse	GCAAGCATAAGACTGGACCAAA
Ppara Forward	GAACGGCTTCCTCAGGTTCTT	*Elovl3* Forward	GGACCTGATGCAACCCTATGA
Ppara Reverse	GCGTACGGCAATGGCTTTAT	*Elovl3* Reverse	TCCGCGTTCTCATGTAGGTCT
Cox7a1 Forward	AGAAAACCGTGTGGCAGAGA	*Ap2* Forward	CCATCTAGGGTTATGATGCTCTTCA

Cox7a1 Reverse	CAGCGTCATGGTCAGTCTGT	*Ap2* Reverse	ACACCGAGATTTCCTTCAAACTG
Prdm16 Forward	GCGTGCATCCGCTTGTG	*Cox2* Forward	GCCTGGGATGGCATCAGTT
Prdm16 Reverse	CAGCACGGTGAAGCCATTC	*Cox2* Reverse	TGAAGACGTCCTCCACTCATGA
Adipoq Forward	GTAGGTGAAGAGAACGGCCTTGT	*Mstn* Forward	AGAAGATGGGCTGAATCCCTT T
Adipoq Reverse	GCACTGGCAAGTTCTACTGCAA	*Mstn* Reverse	ATCGCAGTCAAGCCCAAAGT
Cox5b Forward	CAGCTTGTAATGGGTTCCACAGT	*Trim63* Forward	TCCTGATGGAA ACGCTATGGAG
Cox5b Reverse	GCTGCATCTGTGAAGAGGACAAC	*Trim63* Reverse	ATTCGCAGCCTGGAAGATGT
Cebpa Forward	GTCACTGGTCAACTCCAGCAC	*Myod1* Forward	CGG GAC ATA GAC TTG ACA GGC
Cebpa Reverse	CAAGAACAGCAACGAGTACCG	*Myod1* Reverse	TCG AAA CAC GGG TCA TCA TAG A
Fbxo32 Forward	TCAGAGAGGCAGATT CGCAA	*Erra* Forward	CACTACGGTGTGGCATCCTG
Fbxo32 Reverse	GGGTGACCCCATACTGCTCT	*Erra* Reverse	ACAGCTGTACTCGATGCTCC

SUPPLEMENTARY REFERENCES

1. Guo W, Allan AM, Zong R, Zhang L, Johnson EB, Schaller EG, et al. Ablation of Fmrp in adult neural stem cells disrupts hippocampus-dependent learning. Nat Med. 2011;17(5):559-65.
2. Guo W, Patzlaff NE, Jobe EM, Zhao X. Isolation of multipotent neural stem or progenitor cells from both the dentate gyrus and subventricular zone of a single adult mouse. Nat Protoc. 2012;7(11):2005-12.
3. Sah N, Peterson BD, Lubejko ST, Vivar C, van Praag H. Running reorganizes the circuitry of one-week-old adult-born hippocampal neurons. Scientific Reports. 2017;7(1):10903.
4. Nuber S, Rajsombath M, Minakaki G, Winkler J, Müller CP, Ericsson M, et al. Abrogating Native α-Synuclein Tetramers in Mice Causes a L-DOPA-Responsive Motor Syndrome Closely Resembling Parkinson's Disease. Neuron. 2018;100(1):75-90.e5.
5. Liu B, Hinshaw RG, Le KX, Park MA, Wang S, Belanger AP, et al. Space-like (56)Fe irradiation manifests mild, early sex-specific behavioral and neuropathological changes in wildtype and Alzheimer's-like transgenic mice. Sci Rep. 2019;9(1):12118.
6. Caldarone BJ, Paterson NE, Zhou J, Brunner D, Kozikowski AP, Westphal KG, et al. The novel triple reuptake inhibitor JZAD-IV-22 exhibits an antidepressant pharmacological profile without locomotor stimulant or sensitization properties. The Journal of pharmacology and experimental therapeutics. 2010;335(3):762-70.
7. Shi Q, Colodner KJ, Matousek SB, Merry K, Hong S, Kenison JE, et al. Complement C3-Deficient Mice Fail to Display Age-Related Hippocampal Decline. J Neurosci. 2015;35(38):13029-42.
8. Morris R. Developments of a water-maze procedure for studying spatial learning in the rat. J Neurosci Methods. 1984;11(1):47-60.
9. Vorhees CV, Williams MT. Morris water maze: procedures for assessing spatial and related forms of learning and memory. Nature protocols. 2006;1(2):848-58.
10. Besnard A, Miller SM, Sahay A. Distinct Dorsal and Ventral Hippocampal CA3 Outputs Govern Contextual Fear Discrimination. Cell reports. 2020;30(7):2360-73.e5.
11. Sahay A, Scobie KN, Hill AS, O'Carroll CM, Kheirbek MA, Burghardt NS, et al. Increasing adult hippocampal neurogenesis is sufficient to improve pattern separation. Nature. 2011;472(7344):466-70.
12. Kim WB, Cho J-H. Encoding of contextual fear memory in hippocampal–amygdala circuit. Nature Communications. 2020;11(1):1382.
13. Leger M, Quiedeville A, Bouet V, Haelewyn B, Boulouard M, Schumann-Bard P, et al. Object recognition test in mice. Nature Protocols. 2013;8(12):2531-7.
14. Bilsland JG, Wheeldon A, Mead A, Znamenskiy P, Almond S, Waters KA, et al. Behavioral and Neurochemical Alterations in Mice Deficient in Anaplastic Lymphoma Kinase Suggest Therapeutic Potential for Psychiatric Indications. Neuropsychopharmacology. 2008;33(3):685-700.
15. Wolf A, Bauer B, Abner EL, Ashkenazy-Frolinger T, Hartz AM. A Comprehensive Behavioral Test Battery to Assess Learning and Memory in 129S6/Tg2576 Mice. PloS one. 2016;11(1):e0147733.
16. Faizi M, Bader PL, Saw N, Nguyen T-VV, Beraki S, Wyss-Coray T, et al. Thy1-hAPP(Lond/Swe+) mouse model of Alzheimer's disease displays broad behavioral deficits in sensorimotor, cognitive and social function. Brain and behavior. 2012;2(2):142-54.
17. Choi SH, Bylykbashi E, Chatila ZK, Lee SW, Pulli B, Clemenson GD, et al. Combined adult neurogenesis and BDNF mimic exercise effects on cognition in an Alzheimer's mouse model. Science. 2018;361(6406).
18. Creer DJ, Romberg C, Saksida LM, van Praag H, Bussey TJ. Running enhances spatial pattern separation in mice. Proc Natl Acad Sci U S A. 2010;107(5):2367-72.
19. Young K, Morrison H. Quantifying Microglia Morphology from Photomicrographs of Immunohistochemistry Prepared Tissue Using ImageJ. J Vis Exp. 2018(136).
20. McAvoy KM, Scobie KN, Berger S, Russo C, Guo N, Decharatanachart P, et al. Modulating Neuronal Competition Dynamics in the Dentate Gyrus to Rejuvenate Aging Memory Circuits. Neuron. 2016;91(6):1356-73.
21. Fontaine CJ, Pinar C, Yang W, Pang AF, Suesser KE, Choi JSJ, et al. Impaired Bidirectional Synaptic Plasticity in Juvenile Offspring Following Prenatal Ethanol Exposure. Alcohol Clin Exp Res. 2019;43(10):2153-66.
22. Peñasco S, Rico-Barrio I, Puente N, Gómez-Urquijo SM, Fontaine CJ, Egaña-Huguet J, et al. Endocannabinoid long-term depression revealed at medial perforant path excitatory synapses in the dentate gyrus. Neuropharmacology. 2019;153:32-40.
23. Bannerman DM, Yee BK, Good MA, Heupel MJ, Iversen SD, Rawlins JN. Double dissociation of function within the hippocampus: a comparison of dorsal, ventral, and complete hippocampal cytotoxic lesions. Behavioral neuroscience. 1999;113(6):1170-88.

24. Habib N, Avraham-Davidi I, Basu A, Burks T, Shekhar K, Hofree M, et al. Massively parallel single-nucleus RNA-seq with DroNc-seq. Nature methods. 2017;14(10):955-8.
25. Dobin A, Davis CA, Schlesinger F, Drenkow J, Zaleski C, Jha S, et al. STAR: ultrafast universal RNA-seq aligner. Bioinformatics (Oxford, England). 2013;29(1):15-21.
26. Love MI, Huber W, Anders S. Moderated estimation of fold change and dispersion for RNA-seq data with DESeq2. Genome biology. 2014;15(12):550.
27. Trapnell C, Williams BA, Pertea G, Mortazavi A, Kwan G, van Baren MJ, et al. Transcript assembly and quantification by RNA-Seq reveals unannotated transcripts and isoform switching during cell differentiation. Nature biotechnology. 2010;28(5):511-5.
28. Cornwell M, Vangala M, Taing L, Herbert Z, Koster J, Li B, et al. VIPER: Visualization Pipeline for RNA-seq, a Snakemake workflow for efficient and complete RNA-seq analysis. BMC Bioinformatics. 2018;19(1):135.
29. Huang da W, Sherman BT, Lempicki RA. Systematic and integrative analysis of large gene lists using DAVID bioinformatics resources. Nature protocols. 2009;4(1):44-57.
30. Huang da W, Sherman BT, Lempicki RA. Bioinformatics enrichment tools: paths toward the comprehensive functional analysis of large gene lists. Nucleic acids research. 2009;37(1):1-13.
31. Subramanian A, Tamayo P, Mootha VK, Mukherjee S, Ebert BL, Gillette MA, et al. Gene set enrichment analysis: A knowledge-based approach for interpreting genome-wide expression profiles. Proceedings of the National Academy of Sciences. 2005;102(43):15545.
32. Mootha VK, Lindgren CM, Eriksson K-F, Subramanian A, Sihag S, Lehar J, et al. PGC-1α-responsive genes involved in oxidative phosphorylation are coordinately downregulated in human diabetes. Nature genetics. 2003;34(3):267-73.
33. Benjamini Y, Hochberg Y. Controlling the False Discovery Rate: A Practical and Powerful Approach to Multiple Testing. Journal of the Royal Statistical Society Series B (Methodological). 1995;57(1):289-300.
34. Dempsey GT. A user's guide to localization-based super-resolution fluorescence imaging. Methods Cell Biol. 2013;114:561-92.
35. Schmider AB, Bauer NC, Sunwoo H, Godin MD, Ellis GE, Lee JT, et al. Two- and three-color STORM analysis reveals higher-order assembly of leukotriene synthetic complexes on the nuclear envelope of murine neutrophils. J Biol Chem. 2020;295(17):5761-70.
36. Pageon SV, Nicovich PR, Mollazade M, Tabarin T, Gaus K. Clus-DoC: a combined cluster detection and colocalization analysis for single-molecule localization microscopy data. Mol Biol Cell. 2016;27(22):3627-36.
37. Feher K, Halstead JM, Goyette J, Gaus K. Can single molecule localization microscopy detect nanoclusters in T cells? Curr Opin Chem Biol. 2019;51:130-7.
38. Kim H, Wrann CD, Jedrychowski M, Vidoni S, Kitase Y, Nagano K, et al. Irisin Mediates Effects on Bone and Fat via αV Integrin Receptors. Cell. 2018;175(7):1756-68.e17.
39. Black BJ, Atmaramani R, Pancrazio JJ. Spontaneous and Evoked Activity from Murine Ventral Horn Cultures on Microelectrode Arrays. Frontiers in cellular neuroscience. 2017;11:304-.
40. Everard A, Plovier H, Rastelli M, Van Hul M, de Wouters d'Oplinter A, Geurts L, et al. Intestinal epithelial N-acylphosphatidylethanolamine phospholipase D links dietary fat to metabolic adaptations in obesity and steatosis. Nat Commun. 2019;10(1):457.
41. Ma SM, Chen LX, Lin YF, Yan H, Lv JW, Xiong M, et al. Periostin Promotes Neural Stem Cell Proliferation and Differentiation following Hypoxic-Ischemic Injury. PLoS One. 2015;10(4):e0123585.
42. Markowitz JE, Gillis WF, Beron CC, Neufeld SQ, Robertson K, Bhagat ND, et al. The Striatum Organizes 3D Behavior via Moment-to-Moment Action Selection. Cell. 2018;174(1):44-58.e17.
43. Velasco S, Kedaigle AJ, Simmons SK, Nash A, Rocha M, Quadrato G, et al. Individual brain organoids reproducibly form cell diversity of the human cerebral cortex. Nature. 2019;570(7762):523-7.
44. Bostrom P, Wu J, Jedrychowski MP, Korde A, Ye L, Lo JC, et al. A PGC1-alpha-dependent myokine that drives brown-fat-like development of white fat and thermogenesis. Nature. 2012;481(7382):463-8.

MSSM / AMP-AD analysis

MSSM Differential Expression Results for FNDC5

```
path_base = "~/Dropbox_MGH/Projects/Christiane_Wrann/2020-05_Wrann_APP_PSen1_mouse_hippocampus"
```

```
MSSM_dex = read_tsv(paste0(path_base,"/Consortium analysis MSBB/MSSM_FP_STG_PHG_IFG_DiffExpression.tsv")
```

```
##
## -- Column specification --------------------------------------------------------
## cols(
##   Model = col_character(),
##   Tissue = col_character(),
##   Comparison = col_character(),
##   ensembl_gene_id = col_character(),
##   logFC = col_double(),
##   CI.L = col_double(),
##   CI.R = col_double(),
##   AveExpr = col_double(),
##   t = col_double(),
##   P.Value = col_double(),
##   adj.P.Val = col_double(),
##   B = col_double(),
##   Study = col_character(),
##   Sex = col_character(),
##   hgnc_symbol = col_character(),
##   percentage_gc_content = col_double(),
##   gene.length = col_double(),
##   Direction = col_character()
## )
```

Check available contrasts:

```
table(MSSM_dex$Model, MSSM_dex$Comparison)
```

```
##
##                     1-0    2-0    2-1 AD-CONTROL AD-OTHER    CDR OTHER-CONTROL
##   APOE4           65392  65392  65392          0        0      0             0
##   Diagnosis           0      0      0      65392    65392      0         65392
##   Diagnosis.AOD       0      0      0      65392        0      0             0
##   Diagnosis.Sex       0      0      0     130784        0      0             0
##   SourceDiagnosis     0      0      0          0        0  65392             0
```

Plot FNDC5 p-values for all available contrasts

```
MSSM_dex[grep("FNDC5",MSSM_dex$hgnc_symbol), ]
```

```
## # A tibble: 40 x 18
##    Model     Tissue Comparison ensembl_gene_id    logFC    CI.L     CI.R AveExpr
##    <chr>     <chr>  <chr>      <chr>              <dbl>   <dbl>    <dbl>   <dbl>
```

```
##  1 SourceDi~ FP     CDR        ENSG00000160097  0.00588 -0.0241  0.0359     5.94
##  2 SourceDi~ IFG    CDR        ENSG00000160097 -0.0324  -0.0688  0.00394    5.94
##  3 SourceDi~ PHG    CDR        ENSG00000160097 -0.0854  -0.120  -0.0513     5.94
##  4 SourceDi~ STG    CDR        ENSG00000160097 -0.0640  -0.100  -0.0276     5.94
##  5 Diagnosis FP     AD-OTHER   ENSG00000160097 -0.0816  -0.195   0.0313     5.94
##  6 Diagnosis FP     AD-CONTROL ENSG00000160097  0.00170 -0.134   0.137      5.94
##  7 Diagnosis FP     OTHER-CON~ ENSG00000160097  0.0833  -0.0514  0.218      5.94
##  8 Diagnosis STG    AD-OTHER   ENSG00000160097 -0.214   -0.334  -0.0932     5.94
##  9 Diagnosis STG    AD-CONTROL ENSG00000160097 -0.192   -0.349  -0.0343     5.94
## 10 Diagnosis STG    OTHER-CON~ ENSG00000160097  0.0219  -0.132   0.176      5.94
## # ... with 30 more rows, and 10 more variables: t <dbl>, P.Value <dbl>,
## #   adj.P.Val <dbl>, B <dbl>, Study <chr>, Sex <chr>, hgnc_symbol <chr>,
## #   percentage_gc_content <dbl>, gene.length <dbl>, Direction <chr>
```

```
MSSM_dex %>%
  dplyr::filter(hgnc_symbol == "FNDC5") %>%
  ggplot(aes(x=Comparison,y=-log10(adj.P.Val),colour=Tissue, shape=Study)) +
  geom_point() +
  facet_wrap(~Model, scales="free")
```

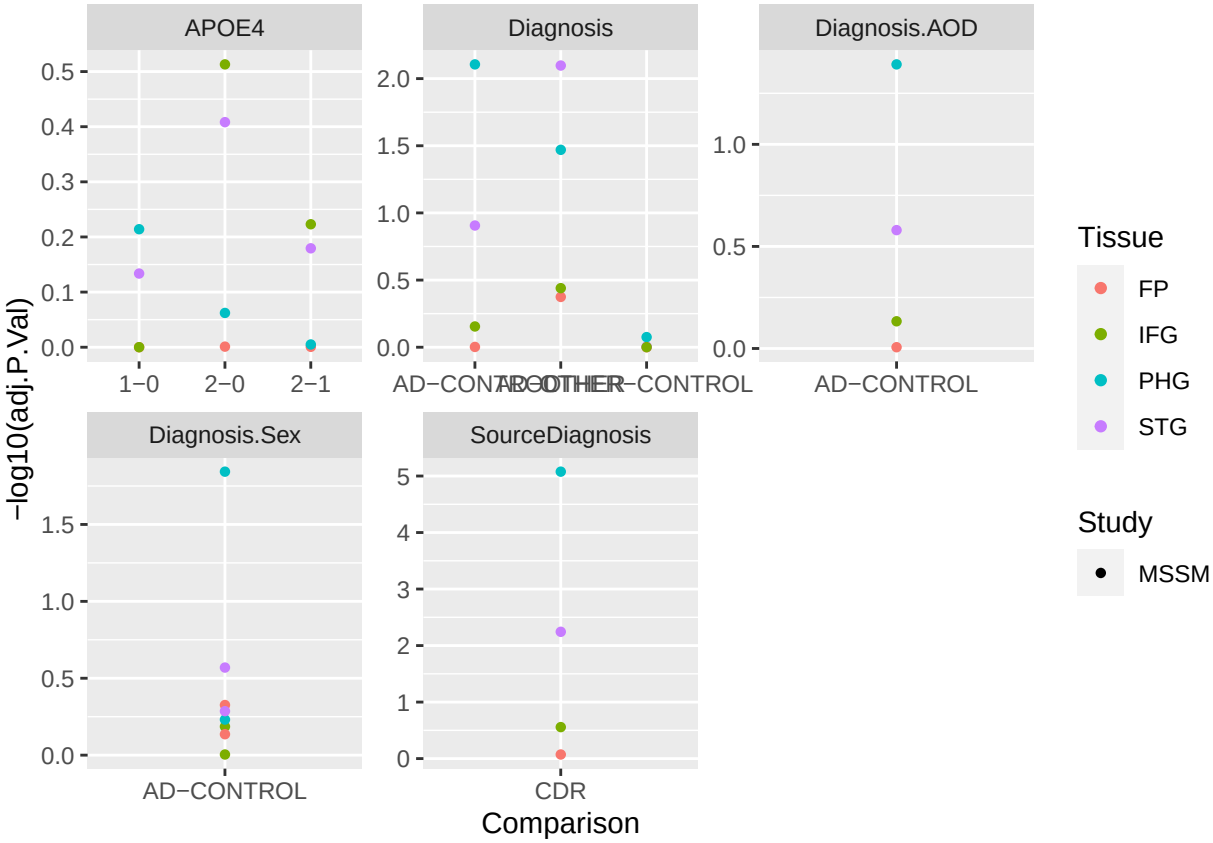

Focus on 'Diagnosis', with AD, CONTROL, and OTHER sample groups:

```
toPlot = MSSM_dex %>%
  dplyr::filter(hgnc_symbol == "FNDC5") %>%
  dplyr::filter(Model == "Diagnosis")

toPlot %>% write.csv(file=paste0(path_base,"/MSSM_data_FNDC5_Dx.csv"), row.names=F)
```

Plot p-values and log2-fold-changes for each contrast:

```r
toPlot %>%
  ggplot(aes(x=logFC,y=-log10(adj.P.Val),colour=Tissue, shape=Study, size=adj.P.Val < 0.05)) +
  geom_hline(yintercept=-log10(0.05)) +
  geom_vline(xintercept=0) +
  geom_point() +
  facet_grid(hgnc_symbol~Comparison, scales="fixed")
```